Two-Dimensional Model of Laser-Sustained Plasmas in Axisymmetric Flowfields

Ronald J. Glumb* and Herman Krier†
University of Illinois, Urbana, Illinois

A two-dimensional numerical model of laser-sustained plasmas in flowing argon has been developed. Real-gas properties and a complete radiation loss mechanism have been included, but radial velocities in the flowfield are neglected. Calculated plasma size, peak temperatures, global absorption characteristics, and thermal efficiencies are in good agreement with experiment. Radiation loss is found to be the dominant process at high laser powers, although thermal conversion efficiencies in excess of 40% (at 20 kW) can be realized by operating at high flow velocities.

Nomenclature

c = speed of light
C_p = specific heat, J/kg·K
D = focus spot diameter, mm
e = electronic charge
f = optical f number
h = Planck constant
I = laser intensity, W/m^2
K = thermal conductivity, W/m·K
k_B = Boltzmann constant
n_e = electron number density, m^{-3}
m_e = electron mass
r = radius, m
t = time, s
T = temperature, K
u,v = axial and radial velocity components, respectively, m/s
z = axial position, m
Z_{eff} = radiation loss correction factor
α = absorption coefficient, 1/m
ϵ = emission coefficient, W/m^3
ρ = density, kg/m^3
ν_C = continuum cutoff frequency, s^{-1}

Introduction

DURING the past several years, investigators have begun to study the use of laser-sustained plasmas (LSP) for application to laser propulsion. As shown in Fig. 1, continuous wave (CW) laser propulsion makes use of a stationary LSP in a steady flow of gas to convert laser energy into the thermal energy of a propellant gas. Such a scheme offers the promise of high specific impulse without sacrificing high thrust capability.[1]

Analytical modeling of laser-sustained plasmas is useful in developing a more complete understanding of the basic physics involved. Phenomena such as absorption efficiencies, radiation losses, and thermal conversion efficiencies are still poorly understood. Modeling can also be used to explore new propellant gases and laser wavelengths that are difficult or currently impossible to study experimentally.

Presented as Paper 85-1551 at the AIAA 18th Fluid Dynamics, Plasma Dynamics and Lasers Conference, Cincinatti, OH, July 14-18, 1985; received July 29, 1985; revision submitted Jan. 24, 1986.

*ONR Fellow, Department of Mechanical and Industrial Engineering.

†Professor of Mechanical Engineering, Department of Mechanical and Industrial Engineering. Associate Fellow AIAA.

The modeling of LSPs began with the one-dimensional work of Raizer.[2] By examining the one-dimensional energy equation with steady flow, he was able to predict wave front velocities and peak temperatures in the LSP. Eventually, the one-dimensional models were expanded to include radiative losses and real-gas properties.[3]

Unfortunately, one-dimensional models have an inherent weakness. LSPs tend to be highly dependent on beam geometry and radial energy transport and are, therefore, clearly two-dimensional phenomena. For this reason, Keefer et al.[4] developed a simplified two-dimensional model that included two-dimensional conduction and radiation loss, but he used a parallel beam and assumed that the radial velocity component of the flow was zero. Also, in order to allow analytical solution, the ratio of specific heat to thermal conductivity C_p/K was assumed to be constant. This approach yielded stable solutions having reasonable peak temperatures and plasma size.

Muller and Uhlenbusch[5] extended Keefer's approach by including a converging beam geometry and a temperature-dependent conductivity function, but again the assumption $C_p/K = \text{const}$ was used. Muller used the results to estimate minimum maintenance powers and found reasonable agreement with experiment, although his values were low because the radiation loss was neglected. More recently, Merkle et al.[6] attempted to produce a more complete model by including the effects of radial flow within the plasma, but his results did not include real-gas properties or a radiation loss mechanism.

The purpose of the present analysis is to extend the steady-state formulation of Keefer to two dimensions using real-gas properties, a converging beam geometry, and a full treatment of the radiative processes. Because many of the properties are highly nonlinear, a numerical solution is required. The only nonrealistic assumption used is that of one-dimensionality in the velocity flowfield. Although this assumption is not technically correct, it is our opinion that radial flow effects are of secondary importance in LSPs. Some experimental evidence supports this conclusion, although more detailed studies are required.[5]

The gas used in the analysis is argon, chosen because of the existence of experimental data with which results can be compared. An additional benefit is that argon has an absorption and radiative behavior similar to that of hydrogen, which is the propellant of choice due to its low molecular weight.

Model Formulation

The two-dimensional cylindrical grid used in the model is shown in Fig. 2. A convergent beam with a "top hat" intensity profile is focused to a variable-size focus point near the axial midpoint, where a steady LSP is maintained in a flow of

argon. It is assumed for convenience that as the beam defocuses, it becomes parallel before striking the side boundary; since little energy absorption takes place in this region, this assumption is unimportant. Argon enters across the upstream boundary at a uniform fixed temperature and at a specified flow velocity. The flow throughout the domain is assumed to be strictly axial; no radial velocity components or radial convection is permitted. The four boundary conditions used are:

1) Symmetry about the $r=0$ cylindrical centerline.

2) Constant conductive heat flux gradient at the outer radial boundary.

3,4) Conduction across the up- and downstream boundaries is negligible compared to the convective transport.

With the assumption of zero radial flow velocity, the continuity equation

$$\frac{\partial}{\partial t}(\rho)+\frac{\partial}{\partial z}(\rho U)+\frac{1}{r}\frac{\partial}{\partial r}(r\rho v)=0 \qquad (1)$$

reduces to the simple equality $\rho u=\text{const}$. With the further assumption of a constant-pressure flowfield, the only equation requiring solution is the two-dimensional energy equation (now decoupled from the momentum equation);

$$\frac{\partial}{\partial z}\left[K\frac{\partial T}{\partial z}\right]+\frac{1}{r}\frac{\partial}{\partial r}\left(rK\frac{\partial T}{\partial r}\right)-\rho uC_p\frac{\partial T}{\partial z}+\alpha I-\epsilon=0 \qquad (2)$$

where I is the laser intensity, α the absorption coefficient, ϵ the emission coefficient, and K the thermal conductivity (which also includes optically thick radiative transport).

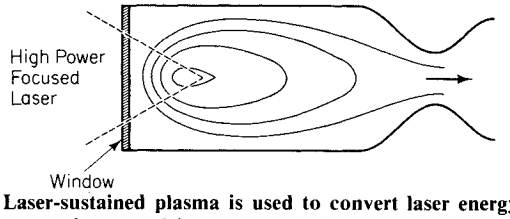

Fig. 1 Laser-sustained plasma is used to convert laser energy into thermal energy for propulsion.

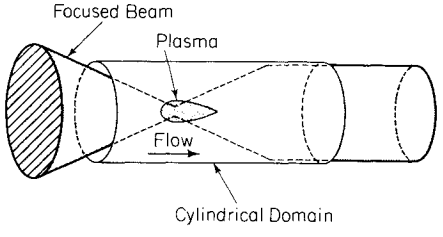

Fig. 2 Cylindrical geometry used in the analysis.

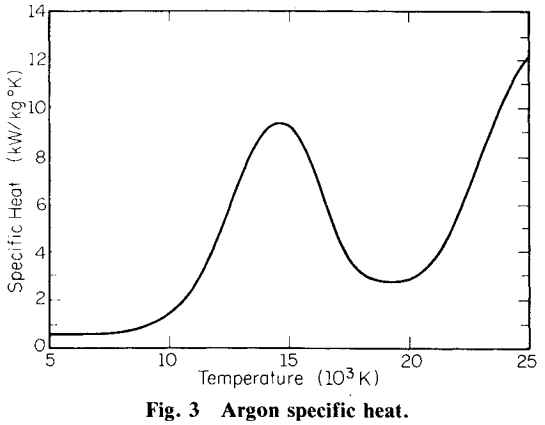

Fig. 3 Argon specific heat.

Solution Procedure

The axially symmetric domain shown in Fig. 2 is divided into a 100×100 network of cells. For this steady-state analysis, the finite differenced form of Eq. 2 is set equal to zero and the temperature of any given cell is written directly as an explicit function of the surrounding cell temperatures and transport properties. However, since most of these properties are highly nonlinear functions of temperature, a direct method of solution is impossible. Instead, a successive over-relaxed Gauss-Seidel iterative procedure is used. Each iteration begins at the upstream radial column of cells and moves downstream. The iterations end when the temperature changes have stopped ($\Delta T/T<10^{-4}$) and when the sum of all energy leaving the domain equals the input laser energy.

As an iteration proceeds downstream, the laser power absorbed by each radial column is subtracted from the incident laser power. Then, this new total power is used to calculate a new beam intensity, taking into account the effect of beam convergence. Because nonuniform absorption across the beam cross section is not accounted for, this simple approach can lead to some error and does tend to slightly overstate the absorption.

Because a valid steady-state solution exists for the condition of $T=300$ K throughout the domain (i.e., no absorption), an initial temperature field must be specified, one that includes

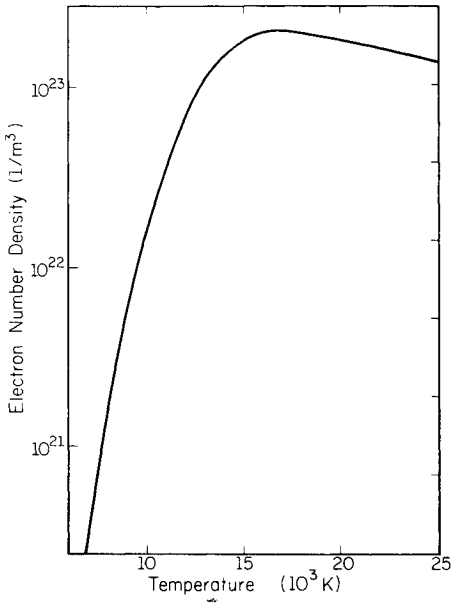

Fig. 4 Argon electron number density.

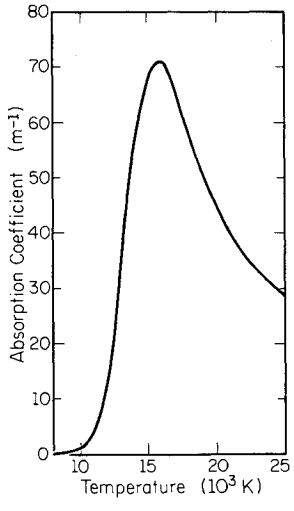

Fig. 5 Argon absorption coefficient.

regions where the gas temperature exceeds the minimum needed for absorption (about 9000 K). The initial temperature field has been determined to have no effect on the final solutions.

For all of the cases run to date, the basic parameters were chosen to match the conditions of the experimental studies now being conducted by the authors.[7] The laser focus diameter is set at 0.8 mm and focusing optics of $f/2.0$ are assumed. The upstream gas temperature is 300 K and an argon flow velocity of 6 cm/s at 1.0 atm pressure is used as the baseline flow rate.

Argon Properties

Throughout the analysis, actual argon properties have been used. Specific heat values are taken from the calculations of Matsuzaki,[8] as shown in Fig. 3. Electron number density values, needed for calculating absorption and emission coefficients, are from the Saha equilibrium calculations of Dresvin[9] and shown in Fig. 4. The 10.6 μm absorption coefficient is calculated following the approach of Wheeler and Fielding[10] and using correction factors developed by Stallcop.[11] The absorption coefficient, plotted in Fig. 5, includes photoionization and electron-ion and electron-neutral inverse bremsstrahlung. The dominant process is *e-i* inverse bremsstrahlung, though the *e-n* process contributes to roughly 40% of the total absorption at intermediate temperatures near 10,000 K.

The thermal conductivity function is less well known. In general, the experimentally measured conductivity agrees well with theory up to only about 10,000 K, at which point the short-range radiative transport within the gas causes the apparent conductivity to rise significantly. Figure 6 shows this discrepancy, with the theoretical curve taken from the work of Sergienko and Fokov[12] and the experimental data from Bues et al.[13] The difference represents the contribution of radiative conductivity. When used in the model, these functions are represented by linearized curve fits; all other properties are approximated by eighth-order curve fits.

Radiation Modeling

To fully model all the radiation transport within an LSP, it is necessary to include three distinct components: short-range optically thick radiation that is quickly reabsorbed by the surrounding gas, radiation loss from the plasma due to continuum free-free and free-bound emission, and radiation loss due to bound-bound line emission. The first of these has already been discussed and can be included in the thermal conductivity function, since its effects are virtually indistinguishable.

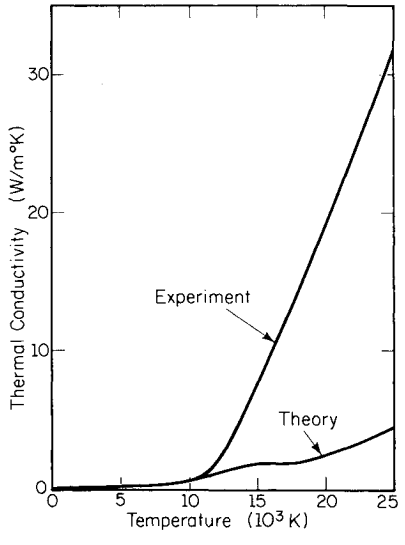

Fig. 6 Theoretical and experimental thermal conductivity functions (the difference is due radiative conductivity).

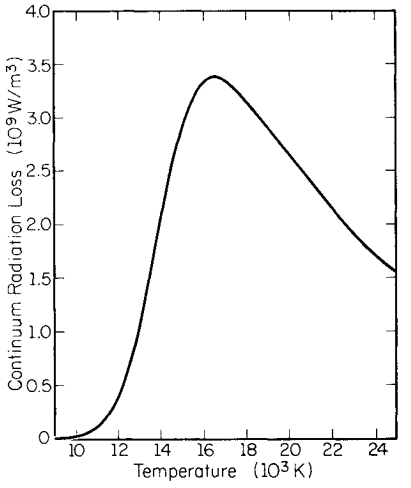

Fig. 7 Argon continuum radiation loss.

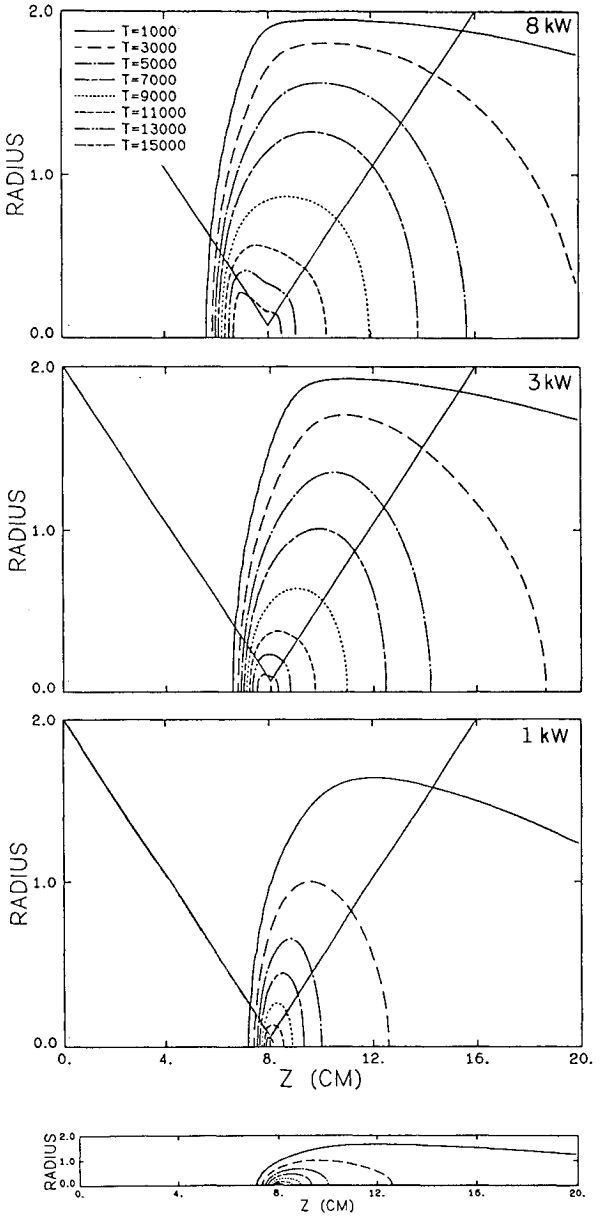

Fig. 8 Isotherm plots of LSP solutions in argon at laser powers of 8, 3, and 1 kW. The plot at bottom illustrates true scale for the 1 kW solution.

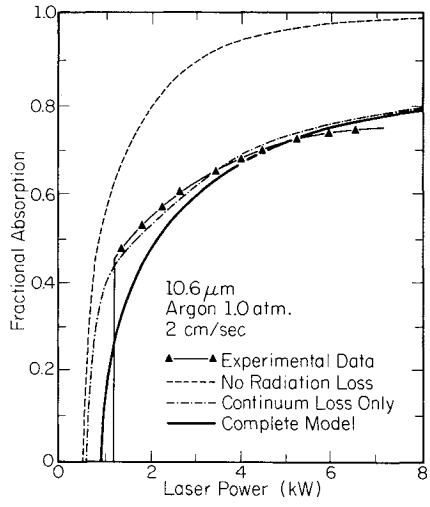

Fig. 9 Experimental global absorption data compared to model predictions.

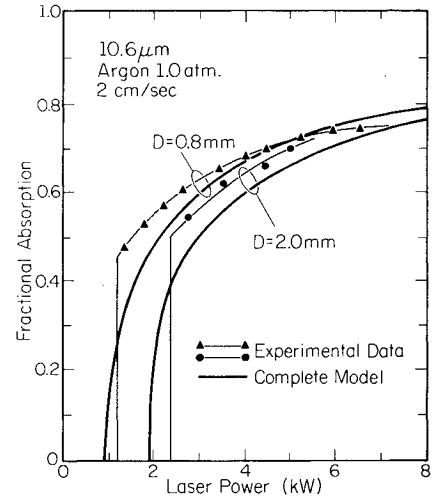

Fig. 10 Global absorption data at two focus spot diameters compared to model predictions.

The continuum emission is treated using the method of Oettinger and Bershader,[14] an approach that has been experimentally verified in argon shock tube studies.[15,16] The expression for this loss, given in W/m^3, is given by

$$q_r = \frac{64e^6\pi^{3/2}}{3c^3 m_e^{3/2}\sqrt{6k_B}} \frac{n_e^2}{\sqrt{T}} \left(\nu_c + \frac{k_B T}{h}\right) Z_{\text{eff}}^2 \qquad (3)$$

where n_e is the electron number density, ν_c the frequency at which the continuum radiation is no longer optically thin (assumed equal to 6.89×10^{14} Hz), and Z_{eff} a correction factor for argon (set equal to 1.225). Since n_e is a known function of temperature, the radiation loss depends only on temperature, as shown in Fig. 7. The radiation loss from each cell is found by multiplying these values by the volume of the cell in question.

The line emission loss term is considerably more complex, since individual emission rates for a number of atomic transitions must be evaluated. At this time, such calculations are still underway and, for the purposes of this study, an alternate approach has been used.

In three independent experimental studies of argon plasmas at densities near 1 atm, each investigator reported that line and continuum radiation contributed nearly equally to the total radiation loss.[14,16] Therefore, in order to approximate the total loss, the continuum loss term has simply been doubled. Although this is not exactly correct, especially since the temperature dependence is slightly different, the error caused by this approximation should not be significant.

Model Results

Using the properties and conditions just discussed, Fig. 8 presents solutions for argon LSPs at laser power settings of 1, 3, and 8 kW. It should be noted that the scale of the vertical axis has been expanded for clarity; the true scale shown at the bottom of Fig. 8 shows that the plasma is actually quite narrow. The solid line on each plot represents the focused beam of the laser.

It can be seen that, as the laser power is reduced, the plasma tends to become smaller and it moves closer to the focus point. This phenomenon has been observed experimentally.[7] In addition, peak temperatures tend to fall, from about 19,000 K in the 8 kW plasma to about 14,000 K at 1 kW. The size of the 3 kW plasma is calculated to be roughly 0.7×4.0 cm. Both the predicted peak temperatures and plasma size agree well with experimental spectroscopic scans of laser-sustained plasmas.[7]

Global Absorption

Another good way to verify the accuracy of a model is to compare the predictions of total absorption by the plasma to experimental data. This tests not only the accuracy of the absorption and emission terms, but also the complex interactions of beam geometry and nonlinear gas properties. Such measurements of global absorption have recently been reported by the authors,[7] the results of which are shown as solid triangles in Fig. 9.

Figure 9 also shows the results of our calculations. Three different sets of predictions are presented to show the effects of different assumptions. The dashed curve at the top assumes no radiation loss and no radiative conductivity. The obvious overestimation of total absorption illustrates the importance of including a radiation loss mechanism.

The curve labeled "continuum loss only" adds the continuum radiation loss to the first curve. Good agreement with the experimental data is evident, although the predicted peak temperatures of over 20,000 K are clearly too high. Finally, the curve labeled "complete model" includes the doubled continuum loss term as well as the radiative conductivity. These two components tend to offset each other. Increasing the radiation loss term reduces the size of the plasma and therefore the overall absorption. But increasing the thermal conductivity enhances heat transfer to the surrounding gas, increasing the size of the plasma while lowering peak temperatures from 20,000-25,000 to 15,000-20,000 K. This drop in core temperature moves the absorption coefficient back into the peak of the absorption curve, as seen in Fig. 5, and increases the overall absorption.

Two other points in Fig. 9 should be noted: 1) the trend predicted by the model closely follows that of the experimental data, and 2) the minimum maintenance power predictions agree well with experiment. Note, however, that experimentally the minimum power is a sharp cutoff, while the model predicts stable solutions where the absorption is as low as 10%. Presumably, a real plasma is susceptible to flow instabilities near its minimum maintenance power that can cause extinguishment.

A second set of experiments is shown in Fig. 10. In this case, a focus diameter of 2.0 mm was used and the results are shown relative to the 0.8 mm data. The model predictions for this larger beam diameter are also presented and indicate good agreement, although the predicted absorption at laser powers below 4 kW is somewhat low.

Thermal Conversion Efficiency

When used for laser propulsion, the main requirement on the LSP is that the conversion of laser energy to exhaust

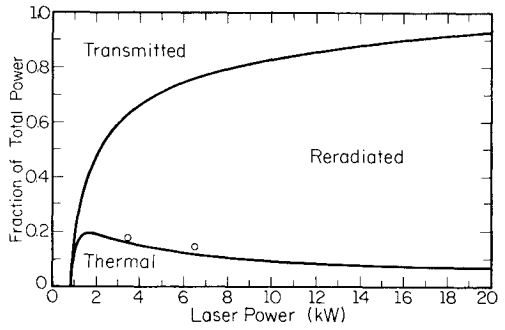

Fig. 11 Fractions of the incident laser power that are transmitted, reradiated, and retained as thermal gas energy.

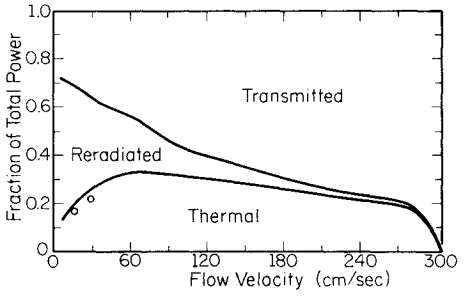

Fig. 12 Fractional powers as functions of flow velocity (laser power is 5 kW; the efficiency peaks at 33%).

kinetic energy be maximized. Figure 11 summarizes our predictions of what happens to the incident laser energy at powers up to 20 kW.

At low laser powers, most of the incident energy is transmitted. Of the remainder, the majority is retained by the gas, since the temperatures within the core are still low enough to inhibit reradiation. But as the laser power is raised and the core temperatures increase, radiation loss from the plasma becomes more significant. The rapidly growing losses quickly cause the percentage retained by the gas to reach a peak and begin falling, in spite of the fact that the overall absorption is still rising. Thus, there appears to be a laser power that will maximize the thermal efficiency of the LSP.

As laser power is increased further, the radiation loss quickly becomes the dominant process. By the time the laser power reaches 20 kW, fully 84% of the incident laser power is reradiated and lost. This is a discouraging result, since it is generally thought that a laser propulsion device must operate at a thermal efficiency of 50% or greater to be practical.

The radiative losses can be controlled to some degree, however, by increasing the mass flow rate. This has the effect of reducing temperatures within the plasma and thus lowering the radiative losses. Unfortunately, this reduction in temperature also lowers global absorption. Both of these effects are evident in Fig. 12, a plot similar to Fig. 11 except that the independent variable is flow velocity.

It is seen that, as the flow velocity increases, radiation losses initially drop faster than global absorption, producing a net increase in the percentage of the incident laser energy retained by the gas. In fact, in this 5 kW case, the thermal gas energy rises from 13% to over 30% before decreasing again as global absorption continues to fall. Therefore, it appears that the thermal efficiency can be maximized by operating at a fairly high flow velocity.

The open circles in Figs. 11 and 12 represent experimentally measured values of thermal efficiency, taken from thermocouple mappings of the flowfield downstream from the plasma.[7] The data indicate good overall agreement, but, more importantly, the predicted trends with flow rate and laser power are both confirmed by the data.

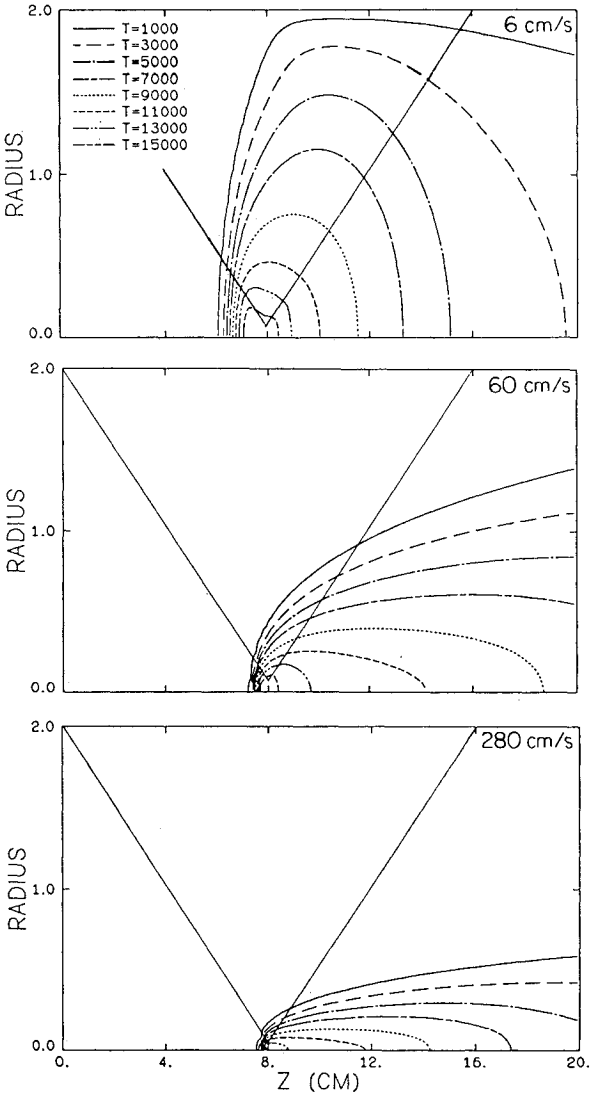

Fig. 13 Isotherm solution plots at flow velocities of 6, 60, and 280 cm/s.

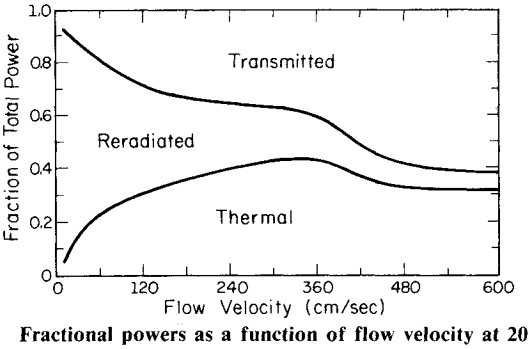

Fig. 14 Fractional powers as a function of flow velocity at 20 kW (peak efficiency has increased to 42%).

The blowout velocity is shown in Fig. 12, which for 5 kW is roughly 300 cm/s. Blowout occurs when the plasma core is forced by high flow rates to move back past the focus point into the diverging portion of the beam, where it cannot be stably maintained. Figure 13 shows the process more clearly, with plots at 6, 60, and 280 cm/s. The final plot is at imminent blowout and illustrates how the plasma is forced into the focal volume just before extinguishing.

An additional series of trials at a laser power of 20 kW are shown in Fig. 14. The trends presented in the 5 kW case are

largely confirmed and a peak in the thermal efficiency is again noted, although at a higher flow rate. The most important trend seen is that the peak efficiency increases from 33% at 5 kW to 42% at 20 kW. This suggests that the maximum achievable efficiency rises with laser power, a significant finding if confirmed at other laser powers.

Conclusions

This new two-dimensional model represents a significant improvement over previous efforts to simulate laser-sustained plasmas in flowing gases. Through the use of real-gas properties and realistic assumptions about radiation losses, excellent agreement with experimental data has been demonstrated. This includes peak temperatures, plasma size, plasma behavior with decreasing power, global absorption data, and beam geometry effects.

It has also been shown that radiation loss becomes the dominant mechanism as the laser power rises. Nevertheless, it is possible to maximize the thermal conversion efficiency through the proper selection of flow velocity. Efficiencies of over 30% are indicated for a power of 5 KW, rising to 42% at 20 kW. Such efficiencies may still be inadequate to justify the complexities inherent in a laser propulsion system, although studies at higher laser powers are required before this question can be answered fully.

The model does have several weaknesses, the most significant being the assumption of zero radial flow velocity. At the extreme temperatures present in LSPs, there will be an outward radial velocity component. However, it is still unclear how significant this effect may be. It may be possible to simulate the radial flow effects by an artificial increase in the conductivity function.

A second shortcoming is the lack of a detailed derivation of the line radiation loss term; in its place, an approximation was used. We are now including such a derivation in the analysis, although we expect only minor deviance from the results presented here. However, it is thought that because the line radiation loss is more dependent on temperature than is the continuum loss, the inclusion of the actual line loss should cause a slight rise in the global absorption values at low laser power.

The final weakness in the model is that the laser beam is assumed to have a "top hat" profile, whereas the laser used in the experiments has an annular cross section. The predicted global absorption at low laser power is expected to rise slightly when the annular beam profile is included in the model, improving the agreement with experimental data.

The logical extension of this work will be to identify operating conditions under which the thermal efficiency can be maximized. The effects of factors such as flow rate, beam geometry, and laser power will be fully explored. In the future, we also hope to extend the model to higher gas pressure and to examine the resultant changes in absorption and emission behavior. Similar studies of LSPs in hydrogen will also be useful.

Acknowledgment

This work is funded by the U.S. Air Force Office of Scientific Research under Grant AFOSR-83-0041. Program Managers are Drs. Leonard H. Caveny and Robert Vondra. The authors also acknowledge the technical discussions and insights provided by Todd Rockstroh of the University of Illinois and Professor Dennis Keefer of the University of Tennessee.

References

[1]Glumb, R.J. and Krier, H., "Concepts and Status of Laser-Supported Rocket Propulsion," *Journal of Spacecraft and Rockets,* Vol. 21, Jan. 1984, pp. 70-79.

[2]Raizer, Y.P., "Subsonic Propagation of a Light Spark and Threshold Conditions for the Maintenance of Plasma by Radiation," *Soviet Physics JETP,* Vol. 31, Dec. 1970, pp 1148-1154.

[3]Kemp, N.H. and Root, R.G., "Analytical Study of Laser-Supported Combustion Waves in Hydrogen," *Journal of Energy,* Vol. 3, Jan. 1979, pp. 40-49.

[4]Keefer, D., Crowder, H., and Elkins, R., "A Two-dimensional Model of the Hydrogen Plasma for a Laser-Powered Rocket," AIAA Paper 82-0404, Jan. 1982.

[5]Muller, S. and Uhlenbusch, J., "Theoretical Model for a Continuous Optical Discharge," *Physica,* Vol. 112C, 1982, pp. 259-270.

[6]Merkle, C.L., Choi, D., and Molvik, G.A., "A Two-dimensional Analysis of Laser Heat Addition in Converging Nozzles," AIAA Paper 84-0529, Jan. 1984.

[7]Krier, H., Mazumder, J., Rockstroh, T.J., Bender, T.D., and Glumb, R.J., "Experimental Studies of Laser-Sustained Plasmas in Argon for Laser Propulsion Applications," AIAA Paper 85-1551, July 1985.

[8]Matsuzaki, R., "Analytical Expressions for Specific Heats and Isentropic Exponent of High Temperature Gases," *Japanese Journal of Applied Physics,* Vol. 21, July 1982, pp. 1003-1008.

[9]Dresvin, S.V., *Physics and Technology of Low Temperature Plasmas,* Iowa State Unversity Press, Ames, 1977.

[10]Wheeler, C.B. and Fielding, S.J., "Absorption of IR Radiation as a General Technique for Determination of Plasma Temperature," *Plasma Physics,* Vol. 12, 1970, pp. 551-564.

[11]Stallcop, J.R., "Absorption Coefficients of a Hydrogen Plasma for Laser Radiation," *Journal of Plasma Physics,* Vol. 11, 1974, pp. 111-129.

[12]Sergienko, A.S. and Fokov, G.A., "Calculation of Characteristics of a Direct Current Argon Arc," *Journal of Engineering Physics,* Vol. 32, April 1977, pp. 399-403.

[13]Bues, I., Patt, H.J., and Richter, J., "Uber die Elektrische Leitfahigkeit und die Warmeleitfahigkeit des Argons bei Hohen Temperaturen," *Zeitschrift fur Angewandte Physik,* Vol. 22, No. 4, March 1967, pp. 345-350.

[14]Oettinger, P.E. and Bershader, D., "A Unified Treatment of the Relaxation Phenomenon in Radiating Argon Plasma Flows," *AIAA Journal,* Vol. 5, Sept. 1967, pp. 1625-1632.

[15]Horn, K.P., Wong, H., and Bershader, D., "Radiative Behavior of a Shock-Heated Argon Plasma Flow," *Journal of Plasma Physics,* Vol. 1, 1967, pp. 157-170.

[16]Logan, P.F., Stalker, R.J., and McIntosh, M.K., "A Shock Tube Study of Radiative Energy Loss from an Argon Plasma," *Journal of Physics D: Applied Physics,* Vol. 1D, 1977, pp. 323-337.